Alignment of the CMS Muon System with Tracks using a HIP-Based Algorithm

Jim Pivarski, Alexei Safonov, Karoly Banicz, Jim Bellinger, Riccardo Bellan

February 8, 2009

1 Introduction and Motivation

show a Z' plot, and say something brief about Heavy Stable Charged Particles
include statement on hardware alignment, how it relates with track-based

2 Geometry of the Muon System and Coordinate Systems

define local x, y, z, ϕ_x, ϕ_y, ϕ_z for DT chambers, for CSC chambers
relate to global $r\phi$, R, and z

3 Description of the Algorithm

The HIP ("Hits and Impact Points") algorithm accumulates residuals distributions for each of the muon chambers, then adjusts the position of each chamber by the offset of the peak of that distribution from zero. When tracks are refitted with the new geometry, residuals should be centered on zero by definition.

A HIP algorithm is also used to align the silicon tracker, but the HIP-based muon alignment algorithm has several important differences, motivated by conditions in the muon system. Each will be covered in its own section below.

3.1 Unbiased Residuals

The globalMuon tracks used for alignment are refitted with normal weights in the silicon tracker but artificially low weights in the muon system (equivalent to an uncertainty-squared of 1000 cm^2), such that the whole path of the refitted trajectory is determined almost entirely by the tracker, yet muon residuals can still be calculated in the normal way. These residuals are unbiased in the sense that the impact point is independent of the hit.

This technique is motivated by two facts about CMS:

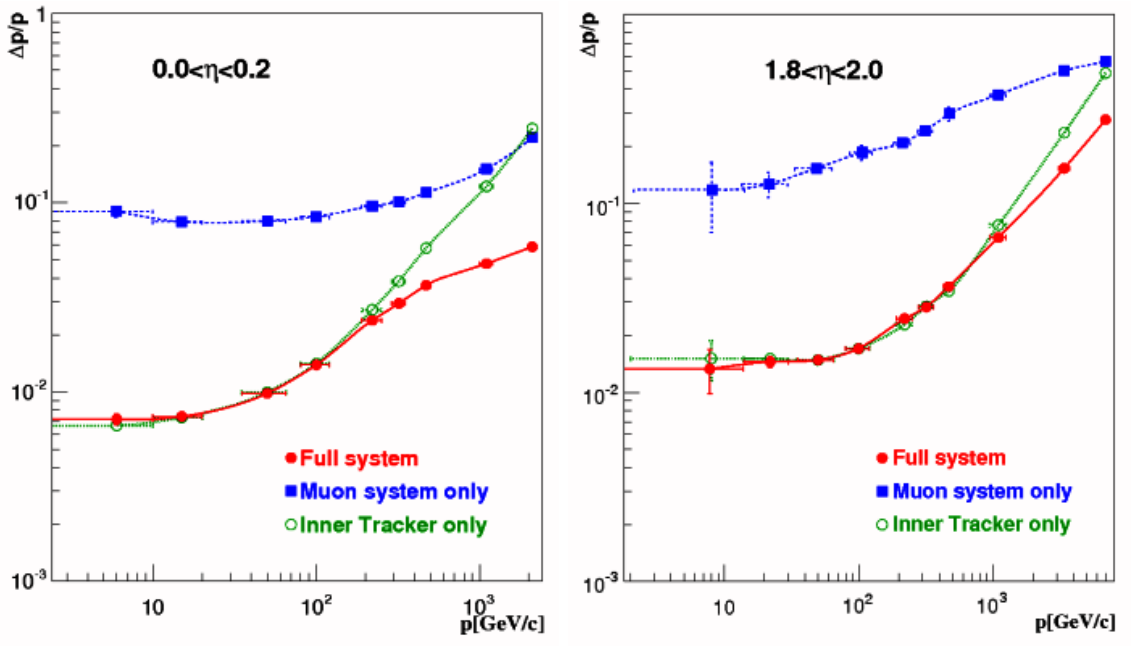

Figure 1: Momentum resolution as a function of momentum. The long lever arm of the muon system becomes a significant advantage for $p_T \gtrsim 200$ GeV, assuming that the muon chambers have been properly aligned.

- the uncertainty in the impact points of tracks propagated through the iron yoke and material in front of the first muon station is on the order of ??? mm due to random scattering in material, and
- silicon tracker hits have a much higher intrinsic resolution than muon chamber hits (??? μm versus 100–300 μm in $r\phi$).

With normal weights, the track fitting algorithm would assume that a large residual in the first hit of a muon chamber is due to scattering in the material through which it propagated and pull the fitted trajectory strongly to the hit. Subsequent hits would have low residuals that do not characterize the misalignment of the chamber. By giving the muon hits low weights, the propagated trajectory instead continues along the path of no scattering. The resulting residuals distributions are wider, but their peaks correspond more exactly to the true misalignment of the chambers.

The second point above implies that this procedure does not lose significant information. Most alignment tracks have a p_T well below 50 GeV, so the muon system's long lever arm plays little role in determining their curvature (Fig. 1). Early tests of the procedure showed that the same alignment resolution was reached by slowly converging with partly-biased residuals as by determining the alignment in one step with unbiased residuals.

Unbiased residuals determine the alignment in one step because there is no coupling between fitting the tracks and updating the muon geometry. The track parameters and full trajectories are independent of the alignment, so the impact points in global coordinates are largely unchanged when the procedure is repeated with a new geometry. We perform a

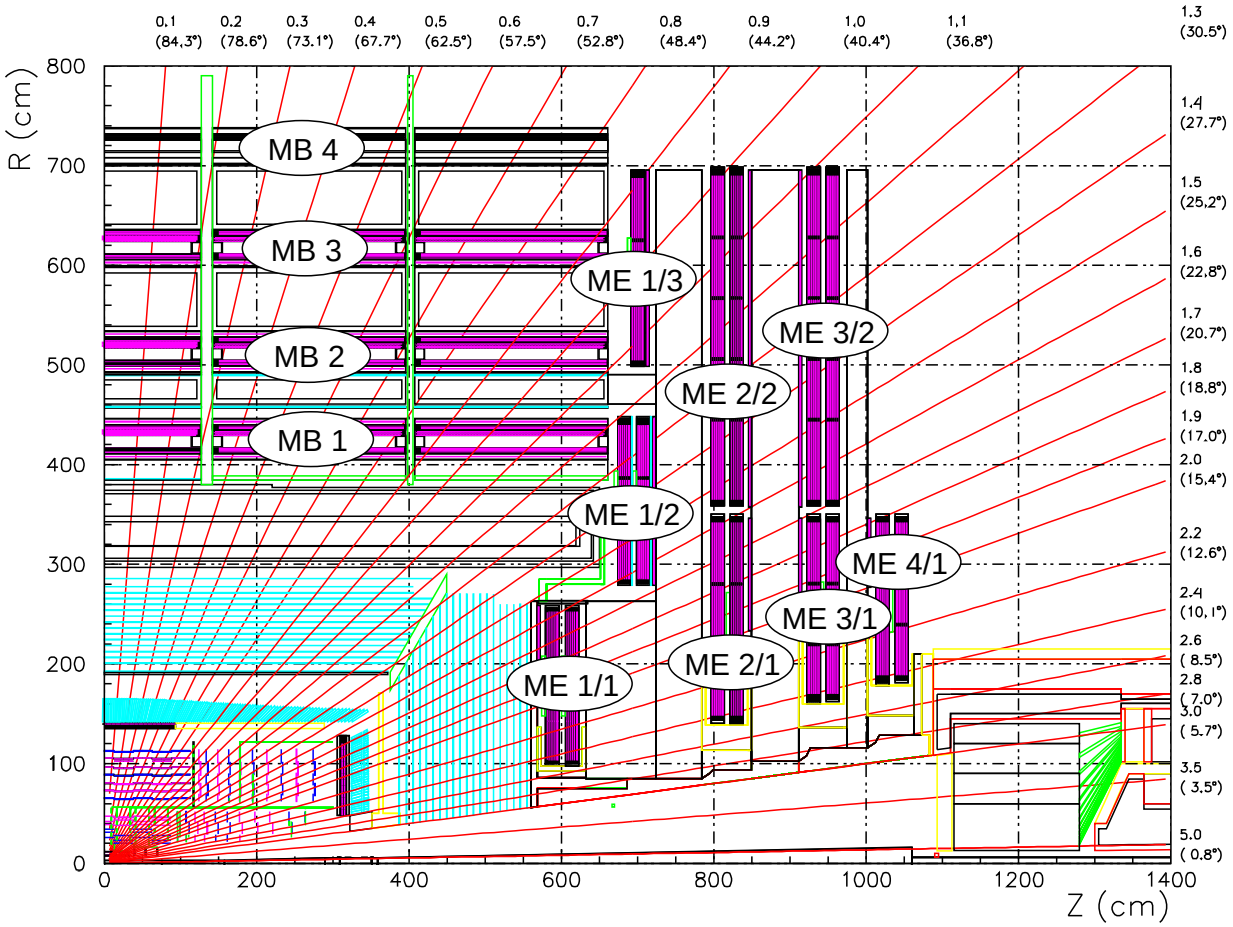

Figure 2: A quarter-view of CMS, labelling the stations of the muon system. "MB" and "ME" specify muon barrel and muon endcap, respectively. The silicon tracker is inside $R < 120$ cm, $|z| < 300$ cm

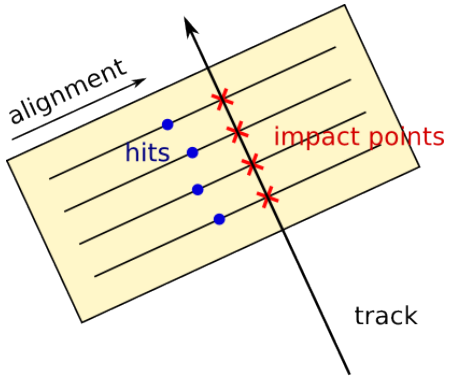

Figure 3: The alignment correction for each chamber is the offset of the peak of its residuals distribution from zero (residual $\equiv$ (impact point) $-$ (hit)). After alignment, the residuals are centered on zero.

second iteration, but only as a verification step. This differs significantly from the tracker alignment procedures, in which gradual convergence is an essential feature of the tracker-HIP algorithm, and the tracker-MillePede algorithm solves a correlated matrix of alignment parameters and track-fitting parameters.

The decoupling is possible because muon alignment is essentially a different problem from alignment of the tracker, in which the shape of the tracker must be determined in isolation. The muon system must be aligned in the same coordinate system as an external reference, the tracker, and we can additionally take advantage of the high precision of that reference to supply us with a fixed set of reference tracks.

3.2 Residuals Peak-fitting Procedure

Also as a consequence of large scattering, the residuals distributions have non-Gaussian tails. Residuals in the tails can pull the mean away from its peak value, where the peak represents the true alignment correction because high-quality tracks agree on the misalignment measurement, and therefore the average residual, while poor-quality tracks (scattering, measurement error) disagree in different ways and don't form a coherent peak. The effect is particularly significant if the shape of the material in front of the muon chamber introduces an asymmetry in this "background" distribution, or if the residuals distribution has low statistics and is susceptible to being pulled by a random sampling of tail events.

To account for the shape of the residuals distribution and to reduce the weight that tail events have in determining the peak, we fit the residuals to a physically-motivated distribution. The fit is unbinned, so there is a sense in which it is a small generalization of simply calculating the mean. The mean, $\sum_{i=1}^{N} r_i/N$, of a set of residuals $\{r_i\}$ is equal to the peak μ of an unbinned Gaussian fit $f(r_i, \mu, \sigma) = \exp(-(r_i - \mu)^2/2/\sigma^2)/\sqrt{2\pi}/\sigma$. What we do differently is to make the fit function more realistic. See Sec. 4.1 for a complete description of the fit function and fitting procedure.

The HIP procedure used to align the tracker determines the peak of each residuals distribution through a weighted mean of residuals (generalized to 6 alignment parameters). The weighted mean reduces sensitivity to scattering in the tracker case, but it would not be effective in our muon alignment procedure because we de-weight the muon hits uniformly in the track fit (see Sec. 3.1).

3.3 Correlation of Hits

The variance in unbiased residuals in a chamber on the same track is much smaller than the variance in unbiased residuals in the chamber, integrated over all tracks. That is to say, the muon hits in a chamber might be widely displaced from their associated track, but they are all closely aligned with each other, because they correspond to the physical path of a real muon, which may be offset from the propagated track because of a scattering event somewhere along its path. Scattering events are unlikely to take place inside the muon chamber because it is mostly a gas volume, and they are much more likely in the iron layers between chambers. The distribution of track errors is also broadened by the fact that the tracks are extrapolations from a distant silicon tracker.

To include all residuals indiscriminantly in a single peak-fit would therefore underestimate the uncertainty in that fit. In the limit of zero intrinsic resolution, each track would encounter N identical residuals, where N is the number of hits per chamber (6, 8, or 12, assuming no inefficiencies). A histogram of these residuals would be an integral multiple of N in every bin and a calculation of its mean or a fit for its peak would have uncertainties underestimated by a factor of $\sqrt{N}$. If we instead average all the residuals on the same track in the same chamber and put the result of that average into the histogram, the uncertainties would be properly estimated. (This relies on the fact that the intrinsic resolution (100–300 μm) is small compared to the distribution of track errors (few mm).)

We can gain additional information by computing a linear fit to the residuals as a function of local z (layer number, accounting for the layer spacings), weighted by intrinsic hit uncertainties. The constant term in this fit plays the same role as the average described above, except that it always represents the hits-impact points discrepancy at the center of the chamber (even with missing hits), the point of the extended chamber body where alignment corrections are applied. The slope contains information about angular misalignment in ϕ_y and ϕ_x (from x and y residuals, respectively). This procedure is similar to calculating residuals with track segments, rather than 1-dimensional hits, except that it only requires the difference of the real and propagated tracks to be linear, not each of them individually, and it benefits from any hit-pruning in the reconstruction of the global track.

[We don't currently do this, though I expect to implement and test it in a matter of days. The CRAFT constants were made with residuals weighted-averaged by chamber, but I want this Note to describe the finalized procedure, since we're close to a full implementation. The angular alignment from these slopes was an important feature of the CSC beam-halo alignment (in ϕ_y).]

3.4 Calculation of Alignment Parameters from Residuals

An offset in the peak of local x and local y residuals from zero clearly correspond to local x and local y translations, but the relationship to local z and angular alignment corrections is more complicated. There are many good ways to do this [reference original HIP paper with Karimaki derivatives], and we have chosen an especially practical and transparent approach. Each parameter is considered independently and computed from uncorrelated variables.

3.4.1 Alignment Parameters for Muon Barrel Chambers

DT chambers have two independent residuals distributions, local x (corresponds to global $r\phi$) from superlayers 1 and 3 and local y (corresponds to global z) from superlayer 2. These 1-dimensional hits are measured independently and are used for independent alignment calculations. Residuals on the same track in the same chamber are combined in a weighted, linear, analytically-calculated fit, as described in Sec. 3.3. The offsets and slopes of these fits are accumulated into two independent residuals distributions. The peak of the "offsets distribution" is determined by the fitting procedure described in Sec. 3.2: the deviation of this peak from zero is the local x or local y alignment correction, depending on whether it was computed from local x or local y residuals. The peak of the "slopes distribution" is

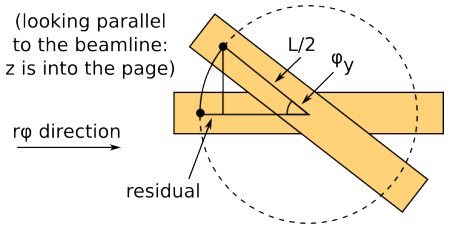

Figure 4: This is way too small to see. Well, maybe not after all the other, larger, effects have been taken care of first.

determined via the same fitting procedure, and its offset from zero is the ϕ_y or ϕ_x angular correction, depending on whether it was computed from local x or local y slopes, respectively.

A slope in local x residuals as a function of local z corresponds to a ϕ_y misalignment for the following reason: when a chamber is rotated around the local y axis, it introduces residuals in the x-z plane that grow linearly with distance from the rotation axis. DT layers can sense x residuals and their z positions are known, and the ratio $\Delta x/\Delta z$ is equal to $\tan\phi_y$ by trigonometry (see Fig. doesn't-exist-yet). The angles are small, so we neglect the tangent. This derivation is exactly the same for ϕ_x angles, swapping the roles of x and y.

In principle, one could also look for ϕ_y and ϕ_x angles in x residuals vs. x and y residuals vs. y, respectively, because the angular rotation would cause the chamber to appear to become narrower. However, this is a second-order effect in the angles (Fig. 4) and a much less-sensitive way of measuring the same thing. [Maybe I shouldn't even have this paragraph and its associated Figure.]

The third angle, ϕ_z doesn't rotate segments, but it does introduce a linear trend in local x residuals as a function of local y and local y residuals as a function of local x. Because DT chambers are longer in the y dimension than the x and also because x residuals are more precise, the local x residual vs. y trend is the most precise way to measure the angle. We split local x derivatives into two bins: one with $y < 0$ and the other with $y > 0$, and compute the peak positions from the "offsets distributions" in each of these independently. The average of the two bins' results is the local x alignment [a minor modification of what was written above], and the difference of the two bins is used to calculate ϕ_z. Specifically,

$$\phi_z = \frac{x \text{ residuals peak in } y < 0 \text{ bin} - x \text{ residuals peak in } y > 0 \text{ bin}}{\text{average } y \text{ of } y < 0 \text{ bin} - \text{average } y \text{ of } y > 0 \text{ bin}}. \quad (1)$$

As a cross-check, we observe y residuals vs. x in our validation plots, to make sure it is also corrected by ϕ_z alignments computed from x residuals vs. y.

Thus we align x, y, ϕ_x, ϕ_y, and ϕ_z using quantities which are not only linearly independent of one another, but orthogonal. There are no correlations between them that would require iteration.

[Local z is special. We need to align the other parameters first, and then possibly iterate with this one. It is not the case that we are insensitive to it; we are sensitive in x residuals vs. x and y residuals vs. y, but only to the degree that the tracks come from a point source. In other words, this is a great collisions-muons measurement, more difficult with cosmic rays.]

3.4.2 Alignment Parameters for Endcap Chambers

Treat CSCs as 1-dimensional residuals (that is, ignore wires), but use the fact that strip measurements are a linear combination of x and y, and that combination varies over the width of the chamber. y will be less sensitive than x this way, but that's all right. Then when we have x and y, we can do all the same tricks as with the DTs. We'll just need to be careful how we organize bins, so that measurements remain uncorrelated.

3.5 Validation Techniques

those plots I've been making

4 Controlling for Systematic Effects

4.1 Tails in Residuals from Scattering Processes

4.2 Momentum-Dependent Residuals from Magnetic Field and Material Budget Errors

The two bins in q/p_T quantifies errors from both a wrong $\vec{B}$-field and a wrong dE/dx. The former is linear in q/p_T, and the latter is very nearly an antisymmetric parabola ($x^3/|x|$). They are both antisymmetric, which makes this safer than a linear fit to the distribution.

[We need to add a cut to reject high p_T events, because charge confusion at high momenta with a non-unit charge ratio makes the two-bin cancellation imperfect. The cut will be about $p_T < 100$ GeV, which is already nearly applied by the cosmics distribution itself.]

4.3 Systematic Errors from Imperfect Tracker Alignment

4.4 Non-uniform illumination

dividing the chamber up into four parts, taking averages; works as long as the distribution of illumination is linear

5 Validation Plots and CRAFT Cosmic Ray Results

6 Simulated Alignment with Collisions

With the up-to-date Summmer08 samples, we can quickly run the finalized procedure on the equivalent of 50 pb^{-1} of inclusive single-muon, and perhaps as much $W^{\pm}$ and Z, thus producing a much more relevant version of the CSA08 study. There will be a new tracker STARTUP scenario (using what they learned from CRAFT) that we can use to quantify dependence on the tracker.

7 Alignment Tools in CMSSW

- Alignment algorithm:
  `Alignment/MuonAlignmentAlgorithms/plugins/MuonAlignmentFromReference`
- Track refitter:
  `TrackingTools/TrackRefitter/plugins/TracksToTrajectories`
- Database comparison and modification tool:
  `Alignment/MuonAlignment/plugins/MuonGeometryDBConverter`
  with full documentation at
  `https://twiki.cern.ch/twiki/bin/view/CMS/SWGuideMuonGeometryConversion`
- Database comparison plots for local differences:
  `Alignment/MuonAlignment/plugins/MuonGeometryArrange`
- Track-based validation:
  `Alignment/CommonAlignmentMonitor/plugins/AlignmentMonitorMuonGeometryMap`
  [not in CVS yet]

8 Conclusions

9 References